

Dalton Transactions

Accepted Manuscript



This is an *Accepted Manuscript*, which has been through the Royal Society of Chemistry peer review process and has been accepted for publication.

Accepted Manuscripts are published online shortly after acceptance, before technical editing, formatting and proof reading. Using this free service, authors can make their results available to the community, in citable form, before we publish the edited article. We will replace this *Accepted Manuscript* with the edited and formatted *Advance Article* as soon as it is available.

You can find more information about *Accepted Manuscripts* in the [Information for Authors](#).

Please note that technical editing may introduce minor changes to the text and/or graphics, which may alter content. The journal's standard [Terms & Conditions](#) and the [Ethical guidelines](#) still apply. In no event shall the Royal Society of Chemistry be held responsible for any errors or omissions in this *Accepted Manuscript* or any consequences arising from the use of any information it contains.

Down-shifting and upconversion photoluminescence in $\text{Ho}^{3+}/\text{Yb}^{3+}$ co-doped GdNbO_4 : effect of Bi^{3+} ion and magnetic field

A. Dwivedi¹, A.K. Singh^{1,2,*}, S.B. Rai¹

¹Department of Physics, Banaras Hindu University, Varanasi-221005, India

²Instituto de Ciencias Físicas, Universidad Nacional Autónoma de México, Cuernavaca, Morelos 62210, México

Abstract

A green emitting $\text{Gd}_{(0.95-x)}\text{Ho}_x\text{Yb}_{0.05}\text{NbO}_4$ phosphor ($x = 0.001, 0.005, 0.01, 0.02, 0.03$ and 0.035) has been synthesized by solid-state reaction method. The phosphor samples were characterized by X-ray diffraction (XRD), Fourier transform infrared (FTIR), Raman and upconversion (UC)/down-shifting (DS) photoluminescence measurements. The XRD analysis confirms the formation of pure phase GdNbO_4 . The FTIR and Raman spectra reveal the modes of vibration in GdNbO_4 . It also confirms that this host has a lower phonon frequency (806 cm^{-1}) in comparison to the other well-known compounds of this family. The photoluminescence excitation (PLE) spectrum of GdNbO_4 shows two broad-bands at 270 and 303 nm corresponding to NbO_4^{3-} group and Gd^{3+} ion, respectively. On 270 nm excitation it shows a weak emission band with maximum at 442 nm, the intensity of this emission band strengthens on excitation with 303 nm. The PL measurements have shown the energy transfer from host to Ho^{3+} ions. In addition, of Bi^{3+} ions, intensity of PL band corresponding to NbO_4^{3-} group increases, which facilitates a better energy transfer from host to the Ho^{3+} ions. On 980 nm diode laser excitation, the phosphor shows strong green and rather weak red UC emission peaks. The influence of external magnetic field on UC emission has also been studied. It is found that UC emission of Ho^{3+} ions decreases in the presence of a magnetic field. It also shows the existence of optical bistability due to the presence of hysteresis behavior. Although this host has a low phonon frequency and shows paramagnetic behavior, yet it is not well explored. Our studies reveal that this host could have significant scientific and technological importance.

Keywords: Upconversion, GdNbO_4 , optical bistability, photoluminescence, charge-transfer band

*Corresponding author: Email: akhilesh_singh343@yahoo.com

1. Introduction

Phosphor, a substance that exhibits luminescence phenomenon, is an important class of material which has large technological applications viz. in cathode ray tube (CRT), plasma video display screens, sensors, white light emitting diodes, *etc.*¹⁻³ It is basically a compound in which transition metal or lanthanide ions are present in traces. Research on lanthanide-based phosphors has been intensified in the last decade for its use in biological applications, photovoltaic, sensor technology, security applications, *etc.*⁴⁻⁶ The prime attraction in the lanthanide-based luminescence materials is due to the presence of sharp emission lines (because of 4f-4f intra-configuration transitions), long lifetime and high color purity.^{7, 8} Due to the presence of a large number of energy states lanthanide has potential to give multimodal luminescence (downshifting (DS), downconversion (DC) and UC emission) from ultra-violet to near-infrared regions. Since, 4f-4f transition in lanthanide are forbidden they show poor absorption cross-section, so a suitable energy sensitization process is needed to increase the luminescence intensity of lanthanide ions.⁹

There are several energy sensitization processes which can enhance the luminescence intensity of lanthanide ions viz by forming lanthanide ion complexes with suitable ligands, by using co-dopent, energy transfer through the charge transfer band, *etc.*^{6,9} Another possible way is to use such host matrices which themselves act as an energy sensitizer for lanthanide ions. These are basically compounds of ABO_4 (where, A is a divalent alkaline earth metal ion or trivalent lanthanide ion and B is a pentavalent or hexavalent transition metal ion) family viz YVO_4 , $CaMoO_4$, YPO_4 , $GdVO_4$, $CaWO_4$, $MgWO_4$, *etc.* Some phosphors derived using these host materials are already explored for several applications. In this family of compounds niobium based host matrices, which show lower phonon frequencies than other compounds of this family, are not well explored. $ANbO_4$ (A= Gd, Y, La) compounds exhibit fergusonite structure and have

good thermal, chemical stability and are environmental friendly.^{10, 11} They emit strong blue emission in UV region on excitation through their charge transfer band. In our previous report, we explored YNbO₄ host matrix for UC emission, using Er³⁺/Yb³⁺ ions, and found that the phosphor is very promising for temperature sensing applications.¹² The objective of this work is to explore some other useful properties of niobium based host matrices. For this we have chosen a GdNbO₄ host in which niobium atoms are tetrahedrally attached with the oxygen atom, in highly distorted site.¹³ Along with the presence of niobate groups (NbO₄)³⁻ which can produce strong blue emission for the sensitization of lanthanide ions, presence of Gd³⁺ can also be used for tuning the luminescence under magnetic field. The effect of magnetic field on luminescence is important for both the fundamental research and various applications such as in distant magnetic field detection.¹⁴ This is yet an under explored area of research.

In the present work we have studied detailed structural and luminescence properties in pure GdNbO₄ and Gd_(0.95-x)Ho_xYb_{0.05}NbO₄ phosphor materials. The Gd_(0.95-x)Ho_xYb_{0.05}NbO₄ phosphor shows strong green emission under UV-Vis and NIR excitation through DS and UC processes. The energy transfer from (NbO₄)³⁻ to Ho³⁺ ion has been verified by excitation, emission and time-domain measurements. We have shown that the presence of small amounts of Bi³⁺ ion changes luminescence behavior, drastically. It enhances the blue emission due to (NbO₄)³⁻ group, three folds. The effect of external magnetic field on the UC emission of Gd_{0.93}Ho_{0.02}Yb_{0.05}NbO₄ phosphor has been studied. It is found that the UC emission intensity decreases as the magnetic field increases. This decrease in the emission intensity is explained by Zeeman splitting. Further, we found the presence of the hysteresis in UC emission intensity verses magnetic field plot which indicates presence of optical bistability in the material.

2. Experimental

2.1 Materials

Analytical reagent grade gadolinium oxide (Gd_2O_3 , 99.9 %, Alfa Aesar), niobium pentaoxide (Nb_2O_5 , 99.95 %, Himedia), ytterbium oxide (Yb_2O_3 , 99.9 %, Alfa Aesar), holmium oxide (Ho_2O_3 , 99.9 %, Molychem) and bismuth oxide (Bi_2O_3 , Molychem) were used for the synthesis of the pure, $\text{Ho}^{3+}/\text{Yb}^{3+}$ and $\text{Ho}^{3+}/\text{Yb}^{3+}$, Bi^{3+} doped GdNbO_4 phosphors.

2.2 Synthesis

GdNbO_4 , $\text{Gd}_{(0.95-x)}\text{Ho}_x\text{Yb}_{0.05}\text{NbO}_4$ ($x = 0.001, 0.005, 0.01, 0.02, 0.03$ and 0.035) and $\text{Gd}_{0.92}\text{Ho}_{0.02}\text{Yb}_{0.05}\text{Bi}_{0.01}\text{NbO}_4$ phosphor samples were prepared by the solid-state reaction method. The stoichiometric amount of raw materials was mixed homogeneously in an agate mortar using AR grade acetone as the mixing media. After the homogeneous mixing, the mixture was placed in an alumina crucible and calcined in high temperature furnace at an optimized temperature 1573 K for 5 h. For UC measurements under a magnetic field, phosphor was used in a pellet form. PVA was used as a binder in making pellets. The pellets were sintered at 1623K in high temperature furnace.

2.3 Characterization

To study the phase purity and crystal structure of phosphor materials, XRD patterns were recorded on 18 kW Cu rotating anode-based high resolution Rigaku powder X-ray diffractometer. Structural analysis was carried out using a Perkin Elmer (Spectrum RX 1) FTIR spectrometer and Reinshaw micro-Raman spectrometer (attached with 514.5 nm Ar^+ laser as an excitation source). For UC emission measurements, a continuous wave diode laser (2W, power tunable) emitting at 980 nm and an iHR 320 (Horiba Jobin Yvon) spectrometer equipped with R928P photomultiplier tube (PMT) was used. PL excitation and emission measurements were

carried out using a Fluorolog-3 spectrofluorometer (Model: FL3-11, Horiba Jobin Yvon) equipped with 450W xenon flash lamp. The lifetime measurements were performed using pulsed xenon lamp (25 W) by the same setup. For optical bistability measurement and to study the effect of magnetic field on UC emission, an electromagnet capable of producing 1(one) tesla high magnetic field was used. The directions of incident light, magnetic field (B) and detection of UC emission were perpendicular to each other. Surface morphology was characterized using scanning electron microscopy (SEM) on ZEISS (SEM-Supra40 model) SEM operated at 20 kV.

3. Results and discussion

3.1 Structural analysis and morphology

The XRD patterns for GdNbO_4 and $\text{Gd}_{0.93}\text{Ho}_{0.02}\text{Yb}_{0.05}\text{NbO}_4$ phosphors are shown in Fig S1. All the diffraction peaks in GdNbO_4 and $\text{Gd}_{0.93}\text{Ho}_{0.02}\text{Yb}_{0.05}\text{NbO}_4$ phosphors can be indexed considering monoclinic structure (space group: $I2$) of GdNbO_4 (JCPDS file: 22-1104). There is no peak corresponding to starting raw materials or impurity phase, suggesting the formation of a pure crystalline phase. This also confirms that $\text{Yb}^{3+}/\text{Ho}^{3+}$ substitutes Gd^{3+} ions in the crystal lattice. To evaluate unit cell parameter in GdNbO_4 and $\text{Gd}_{0.93}\text{Ho}_{0.02}\text{Yb}_{0.05}\text{NbO}_4$ phosphors, Le-Bail analyses of the powder diffraction data have been carried out using crystal structure refinement program "FULLPROF".¹⁵ Peak profiles in the refinement were defined by Pseudo-Voigt function. Figure 1(a) depicts the Le-Bail fit for $\text{Gd}_{0.93}\text{Ho}_{0.02}\text{Yb}_{0.05}\text{NbO}_4$ phosphor using $I2$ space group of monoclinic cell. The refined lattice parameters for GdNbO_4 and $\text{Gd}_{0.93}\text{Ho}_{0.02}\text{Yb}_{0.05}\text{NbO}_4$ phosphors are: $a = 5.3682$ (2)Å, $b = 11.0914$ (5)Å, $c = 5.1040$ (3)Å, $\beta = 94.526$ (3) [R_p = 20.6, R_{wp} = 32.4, R_{exp} = 16.64, $\chi^2 = 3.78$] and $a = 5.3674$ (3)Å, $b = 11.0772$ (6)Å, $c = 5.1039$ (3)Å, $\beta = 94.554$ (4) [R_p = 19.0, R_{wp} = 27.4, R_{exp} = 15.04, $\chi^2 = 3.32$], respectively. The cell volume of $\text{Gd}_{0.93}\text{Ho}_{0.02}\text{Yb}_{0.05}\text{NbO}_4$ is little smaller ($V = 302.77(3)$ Å³) than that of the

GdNbO₄ ($V=302.95(2) \text{ \AA}^3$). This is attributed to the slightly lower ionic radius of Yb³⁺ (86.8 pm) and Ho³⁺ (90.1 pm) than Gd³⁺ (93.8 pm).

As the phonon frequency of the host material is one of the important parameter for getting efficient UC emission, we have studied vibrational features of the GdNbO₄ using Raman and FTIR technique. The Raman spectrum of GdNbO₄ (shown in Fig. 1 (b)) show strong bands at 806 and 328 cm⁻¹ due to the symmetric vibrational mode of Nb-O and weak bands at 665 and 430 cm⁻¹ due to the antisymmetric vibrational mode of Nb-O in NbO₄ tetrahedral structure.^{16, 17} Therefore, the maximum phonon energy in GdNbO₄ is 806 cm⁻¹. If we compare the phonon frequency of GdNbO₄ with other well-known host matrices of ABO₄ family, it is significantly lower. This suggests that GdNbO₄ can be a good host for UC studies which was overlooked from long-time. The FTIR spectra of GdNbO₄ and Gd_{0.93}Ho_{0.02}Yb_{0.05}NbO₄ (shown in Fig 1 (c)) reveal that all the vibrational frequencies are identical. This also confirms the same structure of GdNbO₄ and Gd_{0.93}Ho_{0.02}Yb_{0.05}NbO₄ phosphor. The SEM image, shown in Fig. 1(d), reveals the uniform particle size of Gd_{0.93}Ho_{0.02}Yb_{0.05}NbO₄ phosphor which is of the order of micron (~2 μm).

3.2 Photoluminescence studies

3.2.1 Down-shifting photoluminescence of GdNbO₄ and Gd_(0.95-x)Ho_xYb_{0.05}NbO₄

Host matrices containing a transition metal with no electron in the d-orbital, *viz* compounds with VO₄³⁻, NbO₄³⁻, WO₄²⁻ and MoO₄²⁻ groups, are really useful for phosphor applications. In these matrices, one electron charge-transfer from the oxygen to the empty d-orbital of the central metal ion is involved in the luminescence process.^{12, 13} These phosphors are known as self-activated phosphors. Niobates are known to emit blue light under ultra-violet (UV) and X-ray

excitation. Figure 2 (a) shows PL excitation and emission spectrum of GdNbO₄. The excitation spectrum obtained by monitoring emission at 442 nm wavelength (corresponding to the PL maximum of NbO₄³⁻ group) shows two excitation bands at 270 and 303 nm which corresponds to the NbO₄³⁻ group and Gd³⁺ ion, respectively. The excitation band corresponding to NbO₄³⁻ group in GdNbO₄ is very weak in comparison to the YNbO₄ phosphor. In literature¹⁰ it is reported that in GdNbO₄ the considerable amount of energy absorbed by NbO₄³⁻ group is transferred to the Gd³⁺ ions. Only a very small luminescence is observed by the NbO₄³⁻ group. The Gd³⁺ luminescence, however, are concentrated quenched and lost through the lattice.^{10, 18} In contrast, on excitation with 303 nm, i.e. Gd³⁺ ions, it gives strong luminescence due to NbO₄³⁻ groups which suggest efficient non-radiative energy transfer from Gd³⁺ ions to the NbO₄³⁻ groups. This also brings up doubts on the mechanism stated by earlier workers. Since efficient energy transfer occurs from Gd³⁺ to NbO₄³⁻ groups, it is expected that on 270 nm excitation the energy transferred from NbO₄³⁻ groups to Gd³⁺ ions should be converted to luminescence rather than to lose through lattice vibration.

Figure 2(b) shows PL excitation spectra of Gd_(0.95-x)Ho_xYb_{0.05}NbO₄ phosphor samples observed by monitoring emission at 540 nm corresponding to ⁵F₄/⁵S₂→⁵I₈ transition of Ho³⁺ ion. The sharp peaks at 359, 418 and 449 nm in the PL excitation spectrum corresponds to the ³H₅←⁵I₈, ⁵G₅←⁵I₈ and ⁵G₆←⁵I₈ transitions of Ho³⁺ ion, respectively.¹⁹ It also contains two broad excitation bands at 270 nm and 303 nm is corresponding to NbO₄³⁻ groups and Gd³⁺ ions. The presence of these excitation bands corresponding to NbO₄³⁻ groups and Gd³⁺ and Ho³⁺ ions in the PL excitation spectrum of Gd_(0.95-x)Ho_xYb_{0.05}NbO₄ suggests energy transfer from host to the Ho³⁺ ions. With increasing the Ho³⁺ concentration, intensity of excitation bands increases from x=0.001 to x=0.02, and above this (at x=0.03, 0.035) it starts decreasing. This suggests that

$x=0.02$ is optimum concentration for getting strong PL. The PL excitation spectrum also suggests that the Ho^{3+} ions can be excited directly by excitation into its 4f excited levels or by exciting the bands corresponding to host lattice. Direct excitation of Ho^{3+} ions by 359, 418 and 449 nm radiation gives characteristic emission of Ho^{3+} ions resulting in a greenish color (see Fig. 2(c)). However, when it is excited with 270 or 303 nm radiation (corresponding to the excitation bands of host lattice) it gives broad emission bands corresponding to NbO_4^{3-} group along with characteristic line emission of Ho^{3+} ion (shown in Fig. 2(d)). From Fig. 2(a) and 2(b), it is clear that the emission spectrum of GdNbO_4 overlaps over the excitation spectrum of Ho^{3+} ions, substantially. This facilitates energy transfer from the host to the activator ions.

3.2.2 Effect of Bi^{3+} ion on PL properties of GdNbO_4 and $\text{Gd}_{0.93}\text{Ho}_{0.02}\text{Yb}_{0.05}\text{NbO}_4$

PL of NbO_4^{3-} group is sensitive to the presence of an ion with low-lying energy levels. For example on $\text{Pb}^{2+}/\text{Bi}^{3+}$ ion doping in the phosphor, the 6s electron of $\text{Pb}^{2+}/\text{Bi}^{3+}$ ion is transferred to the empty d-orbital of the niobium ion and the metal to metal charge transfer state becomes the new low-lying emitting state.^{20, 21} Bi^{3+} doped niobate shows two excitation bands: one due to CT transition (2p (O) - 4d (Nb)) at (~280 nm) and other due to CT from 6s (Bi) - 4d (Nb) at (~308 nm). The incorporation of Bi^{3+} into the rare-earth niobates invariably increases the luminescence efficiency. In case of GdNbO_4 the excitation band corresponding to Bi^{3+} to Nb^{5+} CT coincides with the excitation band of Gd^{3+} ions.²² Figure 3(a) shows that in Bi^{3+} doped GdNbO_4 sample both the excitation bands (corresponding to NbO_4^{3-} group and Gd^{3+} ion) are slightly red-shifted. The shift in the excitation band of Gd^{3+} ions is due to the superposition of Bi^{3+} to Nb^{5+} CT band, whereas the shift in excitation band corresponding to NbO_4^{3-} group may be due to slight changes in environment of NbO_4^{3-} group. Furthermore, the intensity of both the excitation bands increased dramatically. The reason behind this is the energy transfer from NbO_4^{3-} group to Bi^{3+}

ion which reduces the possibility of excitation energy losses through Gd^{3+} ion. Blasse¹³ has determined the critical distance for energy transfer between NbO_4^{3-} group to Bi^{3+} ion (2 at. % Bi^{3+} concentration) and Gd^{3+} ion and it is found to be 15Å and 4Å, respectively. Therefore, the possibility of energy transfer from NbO_4^{3-} group to Gd^{3+} is less.

Fig. 3(b) shows the excitation spectrum of $Gd_{0.93}Ho_{0.02}Yb_{0.05}NbO_4$ and $Gd_{0.92}Bi_{0.01}Ho_{0.02}Yb_{0.05}NbO_4$ phosphor obtained by monitoring λ_{em} at 540 nm. Interestingly, Bi^{3+} doped phosphor shows higher intensity of the CT band of host matrix. This suggests that the Bi^{3+} doping increases energy transfer from host lattice to Ho^{3+} ions. This might be due to the increased PL emission in the blue region in Bi^{3+} doped samples. However, the excitation intensity of peaks f-f transition of Ho^{3+} ions decreases significantly on Bi^{3+} doping. This may be due to alternations in the local crystal field environment of Ho^{3+} ions on Bi^{3+} doping. This can also happen due to energy transfer from Ho^{3+} ($^5F_4/^5S_2$) to Bi^{3+} (3P_0) ions, while emission from 3P_0 to the 1S_0 (ground state) in Bi^{3+} ion is forbidden.²³ Fig 3 (c) and (d) shows PL emission spectra of both the samples on excitation with 449 nm and 303/308 nm, respectively. This also reveals the same finding of the excitation spectrum.

The effect of excitation wavelength and Bi^{3+} ions doping on the decay behavior of $^5F_4/^5S_2 \rightarrow ^5I_8$ transition (at 540 nm) has been studied for $Gd_{0.93}Ho_{0.02}Yb_{0.05}NbO_4$ and $Gd_{0.92}Bi_{0.01}Ho_{0.02}Yb_{0.05}NbO_4$ phosphor samples (see Fig. 4). The decay curve of this transition was fitted into single-exponential function as:

$$I(t) = A \exp(-t/\tau),$$

Where, τ is the decay lifetime of the luminescence, and A is the weighting parameter. Fig 4(a) shows decay behavior of $^5F_4/^5S_2 \rightarrow ^5I_8$ transition (540 nm) of Ho^{3+} ions on excitation with 449 nm

(direct excitation of 4f-4f transition) in $\text{Gd}_{0.93}\text{Ho}_{0.02}\text{Yb}_{0.05}\text{NbO}_4$ phosphor. On the mono-exponential curve fitting the lifetime was found to be 48 μs which decreases on Bi^{3+} doping in the phosphor (37 μs). This might be due to the excited state energy transfer from Ho^{3+} to Bi^{3+} ions which was suggested in earlier sections. On the excitation with CT band of the host lattice (303 and 308 nm), lifetime of ${}^5\text{F}_4/{}^5\text{S}_2 \rightarrow {}^5\text{I}_8$ transition is increased from 48 and 37 μs to 452 and 413 μs in $\text{Gd}_{0.93}\text{Ho}_{0.02}\text{Yb}_{0.05}\text{NbO}_4$ and $\text{Gd}_{0.92}\text{Bi}_{0.01}\text{Ho}_{0.02}\text{Yb}_{0.05}\text{NbO}_4$ phosphor samples, respectively.

3.2.3 UC emission studies

The UC emission spectra of $\text{Gd}_{0.98}\text{Ho}_{0.02}\text{NbO}_4$, $\text{Gd}_{0.93}\text{Ho}_{0.02}\text{Yb}_{0.05}\text{NbO}_4$ and $\text{Gd}_{0.92}\text{Bi}_{0.01}\text{Ho}_{0.02}\text{Yb}_{0.05}\text{NbO}_4$ phosphor recorded using 980 nm excitation are shown in Fig 5(a). In the phosphor samples, Ho^{3+} acts as an activator ion, whereas Yb^{3+} used as a sensitizer.²³ It is found that the addition of 5 mole% of Yb^{3+} ions ($\text{Gd}_{0.93}\text{Ho}_{0.02}\text{Yb}_{0.05}\text{NbO}_4$) enhances the UC emission intensity of $\text{Gd}_{0.98}\text{Ho}_{0.02}\text{NbO}_4$ phosphor by ~ 250 folds. The inset to the Fig. 5(a) shows that the maximum UC emission intensity for 2 mole % concentration of Ho^{3+} . The UC emission peaks at 540, 663 and 756 nm can be assigned to ${}^5\text{F}_4/{}^5\text{S}_2 \rightarrow {}^5\text{I}_8$, ${}^5\text{F}_5 \rightarrow {}^5\text{I}_8$ and ${}^5\text{F}_4/{}^5\text{S}_2 \rightarrow {}^5\text{I}_7$ transitions in Ho^{3+} ions, respectively. The ${}^5\text{F}_5$ level is populated by non-radiative relaxation from ${}^5\text{F}_4/{}^5\text{S}_2$ levels. The emission at 756 nm is due to radiative transition from ${}^5\text{F}_4/{}^5\text{S}_2 \rightarrow {}^5\text{I}_7$ followed by non-radiative transitions from ${}^5\text{I}_7$ to ${}^5\text{I}_8$ level. The energy gap between the ${}^5\text{F}_4/{}^5\text{S}_2$ and ${}^5\text{F}_5$ level and ${}^5\text{I}_7$ and ${}^5\text{I}_8$ is about 3000 and 4500 cm^{-1} , respectively. Thus, it requires 4-5 phonons relaxation. Therefore the probability of these non-radiative relaxation is small.²⁴ This is the reason why red emission is very weak in comparison to green UC emission in this host. Interestingly, in other hosts viz. YVO_4 , CaMoO_4 and CaWO_4 belonging to this family of compounds, the intensity of red emission peak is higher than the green emission bands because

of higher phonon frequency and non-radiative relaxation.²⁵ This suggests that GdNbO₄ is a good host for UC. It can be seen from the Fig. 5(a) that the Bi³⁺ doping here again decreases UC emission intensity. The reason behind this is same as the explained in the section 3.2.2.

The power dependence of the UC emission intensity of Gd_{0.93}Ho_{0.02}Yb_{0.05}NbO₄ is shown in Fig 5(b). The $\ln P$ - $\ln I$ plot was fitted in straight line emission corresponding to 540 and 663 nm peaks. The slopes of lines which describe the number of photons involved in the particular UC emission peak are found to be 1.76 and 1.62 for 540 and 663 nm peaks, respectively. This clearly indicates the involvement of two photons in the UC emission. The deviation in the slope values corresponding to 540 and 663 nm UC emission bands from rounded up value 2 is due to the simultaneous involvement of different mechanisms viz excited state absorption (ESA), energy transfer and non radiative relaxations, *etc.*²⁶ The slope in both the cases decreases at higher pump power and show a tendency towards saturation. This is because of the fact that at the higher pump power the levels are highly populated and a part of the energy is dissipated through the lattice vibration. Further, Suyver *et al.*²⁷ have proposed that at high pump power limit, the emission from a particular state to ground state is insignificant, whereas the UC process to the next higher level from that particular level is significant. Therefore, at high power limit slope approaches to unity.

In Ho³⁺ ions, since there is no any resonant level corresponding to 980 nm excitation, the nearest lying levels (⁵I₅, ⁵I₆) are populated through phonon assisted ground state absorption process. The ⁵I₆ level has a comparatively higher lifetime (of the order of ms), therefore the ions in this level reabsorb the incident photons (ESA) and populate the higher lying levels (⁵S₂/⁵F₄). As the number of ions in ⁵I₆ is small, the emission intensity from these levels is also small. However, if Yb³⁺ are also present in the phosphor, due to a higher absorption cross-section of

Yb^{3+} ions for the 980 nm wavelength, large number of Yb^{3+} ions are promoted to the excited state. These excited Yb^{3+} ions transfer their energy to the Ho^{3+} ions present in the ground state and populate $^5\text{I}_6$ state strongly. The ions in $^5\text{I}_6$ level absorb incident photon (ESA) and promoted to $^5\text{F}_4/^5\text{S}_2$ levels as shown in fig. 6. The $^5\text{F}_4/^5\text{S}_2$ levels are also populated directly through a cooperative process of Yb^{3+} ions. The probability of three photon absorption in Ho^{3+} is very less; therefore the blue emission in Ho^{3+} is rarely observed and has very weak intensity.

3.3 Effect of magnetic field on UC luminescence intensity

The materials in which luminescence and magnetic property simultaneously exist are very few in nature and have potential applications in magnetic resonance imaging (MRI) contrast, high-accuracy communications, magnetic field detection, and biological applications (drug and gene delivery, bio-sensing and hyperthermia application).^{14, 28-30} Therefore, it is imperative to investigate such materials. These materials can be produced by making a composite of luminescent materials and magnetic ones³⁰ or by synthesizing a single phase material in which both luminescence and magnetic properties simultaneously exist.²⁹⁻²⁹ The latter is preferred over former because due to the separation between optical and magnetic phases it is difficult to realize an interaction between the optical and magnetic properties in composite material. Lanthanide ions doped gadolinium matrices viz. $\text{NaGdF}_4:\text{Yb}^{3+},\text{Er}^{3+}$, $\text{Gd}_2\text{O}_3:\text{Yb}^{3+},\text{Er}^{3+}$ have been used for this purpose.²⁸⁻²⁹

It is well known that in lanthanide doped crystalline host matrices, due to crystal field the degeneracy of energy levels is removed and a splitting is seen in the levels. When these materials are placed in a magnetic field (weak field) these levels further splits due to the Zeeman Effect. To know the effect of magnetic field on the UC emission behavior we excited

$\text{Gd}_{0.93}\text{Ho}_{0.02}\text{Yb}_{0.05}\text{NbO}_4$ phosphor with 980 nm wavelength under magnetic field. As discussed earlier (section 3.2.3) on excitation with 980 nm radiation, $^5\text{F}_4/^5\text{S}_2$ levels are populated and they give intense emission in the green region. The intensity of the green line decreases with the magnetic field (see Fig. 7). This is because of the fact that under magnetic field the energy level splits due to Zeeman Effect and there is no resonant level of excitation. Thus the population of $^5\text{F}_4/^5\text{S}_2$ levels decrease with increasing magnetic field and so is the intensity of the lines emitted from these levels. A similar finding was also reported by Tikhomirov *et al.*¹⁴ and Singh *et al.*²⁸ in the Er^{3+} doped glass-ceramic and phosphor, respectively. When we decrease the magnetic field keeping the pump power same, the UC emission intensity though increase but does not follow the same path, but it show a hysteresis loop (see Fig. 7). The presence of hysteresis loop indicates the existence of optical bi-stability in the phosphor.²⁸ Tsunekawa *et al.*³¹ have reported that the GdNbO_4 which is a ferroelastic material also shows paramagnetic behavior. We hope that the interaction between the induced magnetization in the GdNbO_4 host and intrinsic magnetic moment of the Ho^{3+} and Yb^{3+} ions is responsible for optical bi-stability in this phosphor. The Ho^{3+} and Yb^{3+} ion pairs form nanosized clusters in the phosphor which acts as nanodomains. Thus, the applied magnetic field causes induced magnetization in the host, resulting Zeeman splitting in the levels due to which the UC emission intensity decreases. On removal of the magnetic field, because of the paramagnetic behavior of GdNbO_4 the induced magnetization of the host becomes zero, but still there is some residual magnetization in the nanodomains.²⁴ This residual magnetization in the nanodomains is responsible for the hysteresis behavior.

4. Conclusions

$\text{Gd}_{(0.95-x)}\text{Ho}_x\text{Yb}_{0.05}\text{NbO}_4$ phosphor shows strong visible emission through DS/UC processes and behaves as a dual-mode phosphor. On UV excitation, GdNbO_4 shows strong blue emission corresponding to NbO_4^{3-} group. This emission is found to enhance further in the presence of small amounts of Bi^{3+} ions. The PL excitation and emission shows energy transfer from the host lattice to the Ho^{3+} ions. On excitation with 980 nm diode laser it gives strong green UC emission which proves the potential of this host. The addition of Bi^{3+} ion in traces in this case reduces the UC emission this might be due to the energy transfer from Ho^{3+} to Bi^{3+} or change in crystal symmetry around Ho^{3+} ions. A decrease in UC emission intensity is observed in the presence of a magnetic field. It could be explained to be due to Zeeman splitting. The results also show that this material can be used for sensing magnetic field also as magneto-optic modulators.

Author Contributions

The manuscript was written through the contributions of all authors. A.D. and A.K.S. have contributed equally to this work and both are the first author of this manuscript. All the authors have given approval to the final version of the manuscript.

Acknowledgements

Authors thankfully acknowledge the support from Prof. Ranjan Kumar Singh and Prof. P.C. Srivastava for Raman and UC measurements under a magnetic field, respectively. A. Dwivedi acknowledges UGC, India for the award of RFSMS meritorious fellowship. A. K. Singh thankfully acknowledges financial support by UGC, India (Dr. D. S. Kothari postdoctoral fellowship (No. F. 4-2/2006 (BSR)/13-906/2013 (BSR)) from April 2013 to February 2014) and UNAM, Mexico (DGAPA, started from March 2014) in the form of postdoctoral fellowship.

Electronic Supplementary Information (ESI) available: X-ray diffraction patterns of GdNbO_4 and $\text{Gd}_{0.93}\text{Ho}_{0.02}\text{Yb}_{0.05}\text{NbO}_4$ are given in ESI.

Reference

1. Z. Xia and R. Lui, *J. Phys. Chem. C*, 2012, **116**, 15604-15609.
2. C. R. Ronda, *J. Alloys and Comp.*, 1995, **225**, 534-538.
3. C. H. Kim, I. E. Kwon, C. H. Park, Y. J. Huang, H. S. Bae, B. Y. Yu, C. H. Pyun and G. Y. Hong, *J. Alloys and Comp.*, 2000, **311**, 33-39.
4. G. Yi, H. Lu, S. Zhao, Y. Ge, W. Yang, D. Chen and L. H. Guo, *Nano Letters*, 2004, **4**, 2191-2196; Y. Dwivedi, A.K. Singh, R. Prakash, S.B. Rai, *J. Lumin.* 131 (2011) 2451–2456.
5. H. Q. Wang, M. Batentschuk, A. Osvet, L. Pinna and C. J. Bradec, *Adv. Mater.*, 2011, **23**, 2675-2680.
6. C. Joshi, A. Dwivedi and S. B. Rai, *Spectrochim. Acta A*, 2014, **129**, 451-456; A. K. Singh, S. K. Singh and S. B. Rai, *RSC Adv.*, 2014, **4**, 27039-27061.
7. F. Auzel, *Chem. Rev.*, 2004, **104**, 139-173.
8. G. Blasse and B. C. Grabmaier; *Luminescent Materials*, Springer-Verla, Berlin, Heidelberg, 1994, Chapter-485.
9. A. K. Singh, S. K. Singh, R. Prakash and S. B. Rai, *Chem. Phys. Lett.*, 2011, **485**, 309-314; A. K. Singh, S. K. Singh, H. Mishra, R. Prakash and S. B. Rai, *J. Phys. Chem. B*, 2010, **114**, 13042-13051.
10. G. Blasse and A. Bril, *J. Lumin.*, 1970, **3**, 109-131.
11. Y. Lü, X. Tang, L. Yan, K. Li, X. Liu, M. Shang, C. Li and J. Lin, *J. Phys. Chem. C*, 2013, **117**, 21972-21980.

12. A. K. Singh, S. K. Singh, B. K. Gupta, R. Prakash and S. B. Rai, *Dalton Trans.*, 2013, **42**, 1065-1072.
13. G. Blasse, *J. Lumin.*, 1976, **14**, 231-233.
14. V. K. Tikhomirov, L. F. Chibotaru, D. Saurel, P. Gredin, M. Mortier and V. V. Moshchalkov, *Nano Letters*, 2009, **9**, 721-724.
15. J. Rodriguez-Carvajal, FULLPROF: A Rietveld and Pattern Matching Analysis Program, Laboratoire Leon Brillouin(CEA-CRNS), France, 2007.
16. G. Blasse, *J. Solid State Chem*, 1973, **7**, 169-171.
17. M. Nazarov, Y. J. Kim, E. Y. Lee, M. S. Jeong, S. W. Lee and D. Y. Noh, *J. Appl. Phys.*, 2010, **107**, 103104(1-6).
18. D. A. Grisafe and C. W. Fritsch, *J. Solid State Chem.*, 1976, **17**, 313-318.
19. A. Pandey and V. K. Rai, *Dalton Trans.*, 2013, **42**, 11005-110011.
20. M. Weigel, W. Middel and G. Blasse, *J. Mater. Chem.*, 1995, **5**, 981-983.
21. X. Jing, C. Gibbons, D. Nicholas, J. Silver, A. Vecht and S. Frampton, *J. Mater. Chem.*, 1999, **9**, 2913-2918.
22. X.M. Liu and J. Lin, *J. Lumin.*, 2007, **122–123**, 700–703.
23. C. Hazra, S. Sarkar and V. Mahalingam, *RSC Adv.*, 2012, **2**, 6926-6931.
24. A. Pandey, V. K. Rai, R. Dey and K. Kumar, *Mat. Chem. Phys.*, 2013, **139**, 483-488.
25. A. K. Singh, S. K. Singh, P. Kumar, B. K. Gupta, R. Prakash and S. B. Rai, *Sci. Adv. Mater.*, 2014, **6**, 405-412; J. H. Chung, J. H. Ryu, S. W. Mhin, K. M. Kim and K. B. Shim, *J. Mater. Chem.*, 2012, **22**, 3997-4002; H. Cho, J. Lee and J. H. Ryu, *9th International Conference on Fracture & Strength of Solids*, June 9-13, 2013, 1-7, Jeju, Korea.

26. R. Dey and V. K. Rai, *Dalton Trans.*, 2014, **43**, 111-118.
27. J. F. Suyver, A. Aebischer, S. G. Revilla, P. Gerner and H. U. Güdel, *Phys. Rev. B*, 2005, **71**, 125123.
28. S. K. Singh, K. Kumar, M. K. Srivastava, D. K. Rai and S. B. Rai, *Optics Letters*, 2010, **35**, 1575.
29. Y. Liu, D. Wang, J. Shi, Q. Peng and Y. Li, *Angew. Chem. Int. Ed.* 2013, **52**, 4366–4369.
30. A. I. Prasad, A. K. Parchur, R. R. Juluri, N. Jadhav, B. N. Pandey, R. S. Ningthoujam and R. K. Vatsa, *Dalton Trans.*, 2013, **42**, 4885-4896.
31. S. Tsunekawa, H. Yamauchi and Y. Yamaguchi, *J. Alloy Comp.*, 1993, **192**, 108-110.

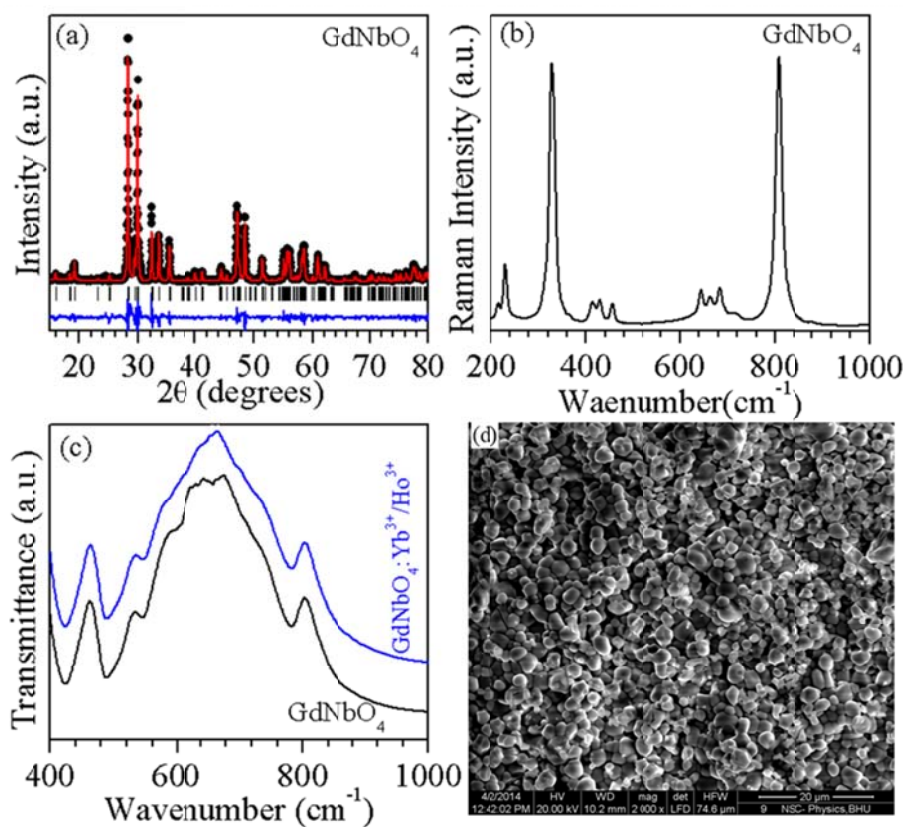


Figure 1: (a) Observed (dots), calculated (continuous line), and difference (bottom line) profiles obtained after Le-bail fitting of $\text{Gd}_{0.93}\text{Ho}_{0.02}\text{Yb}_{0.05}\text{NbO}_4$ using $I2$ space group of monoclinic cell. Vertical tick marks above the difference plot show the positions of the Bragg peaks. (b) Raman spectrum of GdNbO_4 . (c) FTIR spectrum of GdNbO_4 and $\text{Gd}_{0.93}\text{Ho}_{0.02}\text{Yb}_{0.05}\text{NbO}_4$ phosphor. (d) SEM image of $\text{Gd}_{0.93}\text{Ho}_{0.02}\text{Yb}_{0.05}\text{NbO}_4$ phosphor.

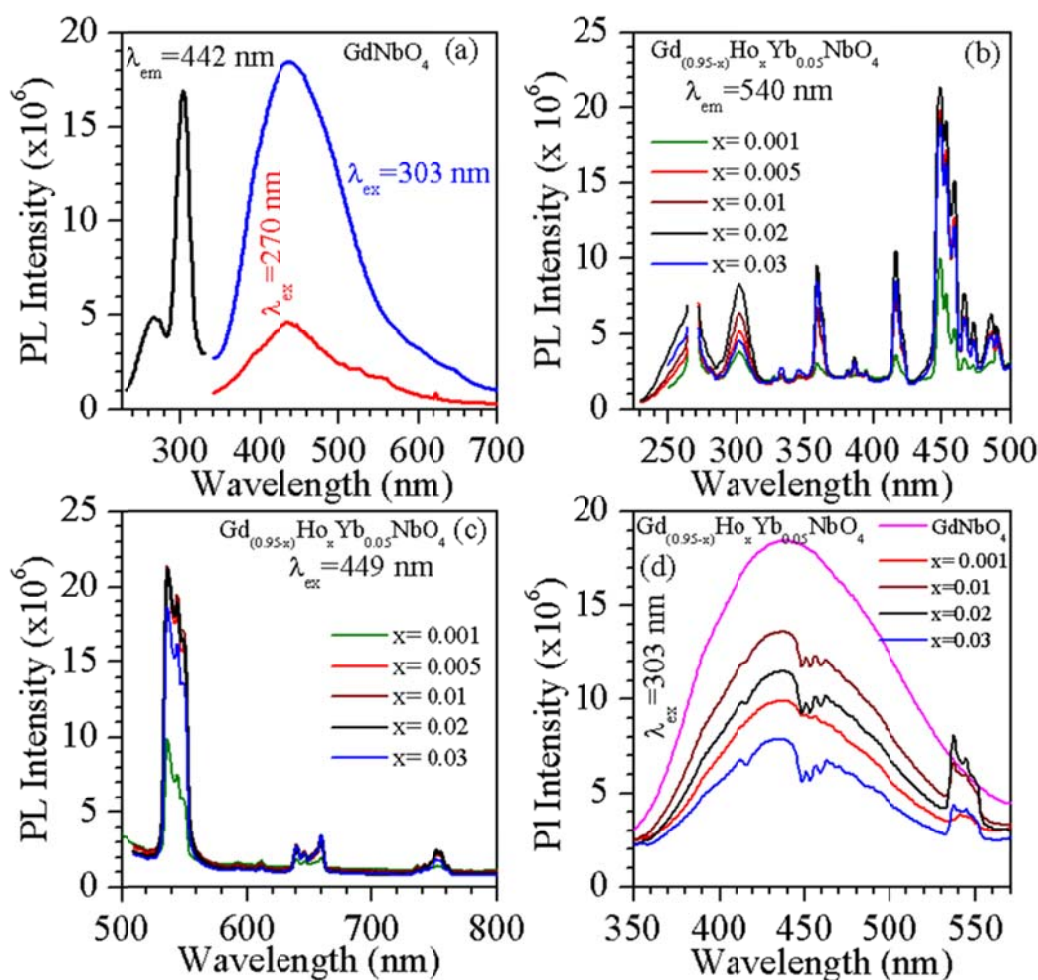


Figure 2: (a) PL excitation and emission spectra of GdNbO₄ monitored at $\lambda_{em} = 442$ nm and $\lambda_{ex} = 270$ and 303 nm, respectively. (b) PL excitation spectra of Gd_(0.95-x)Ho_xYb_{0.05}NbO₄ recorded at $\lambda_{em} = 540$ nm, for $x = 0.001, 0.005, 0.01, 0.02$ and 0.03 . (c) PL emission spectra of Gd_(0.95-x)Ho_xYb_{0.05}NbO₄ recorded at $\lambda_{ex} = 449$ nm, for $x = 0.001, 0.005, 0.01, 0.02$ and 0.03 . (d) PL emission spectra of GdNbO₄ and Gd_(0.95-x)Ho_xYb_{0.05}NbO₄ recorded at $\lambda_{ex} = 303$ nm, for $x = 0.001, 0.01, 0.02$ and 0.03 .

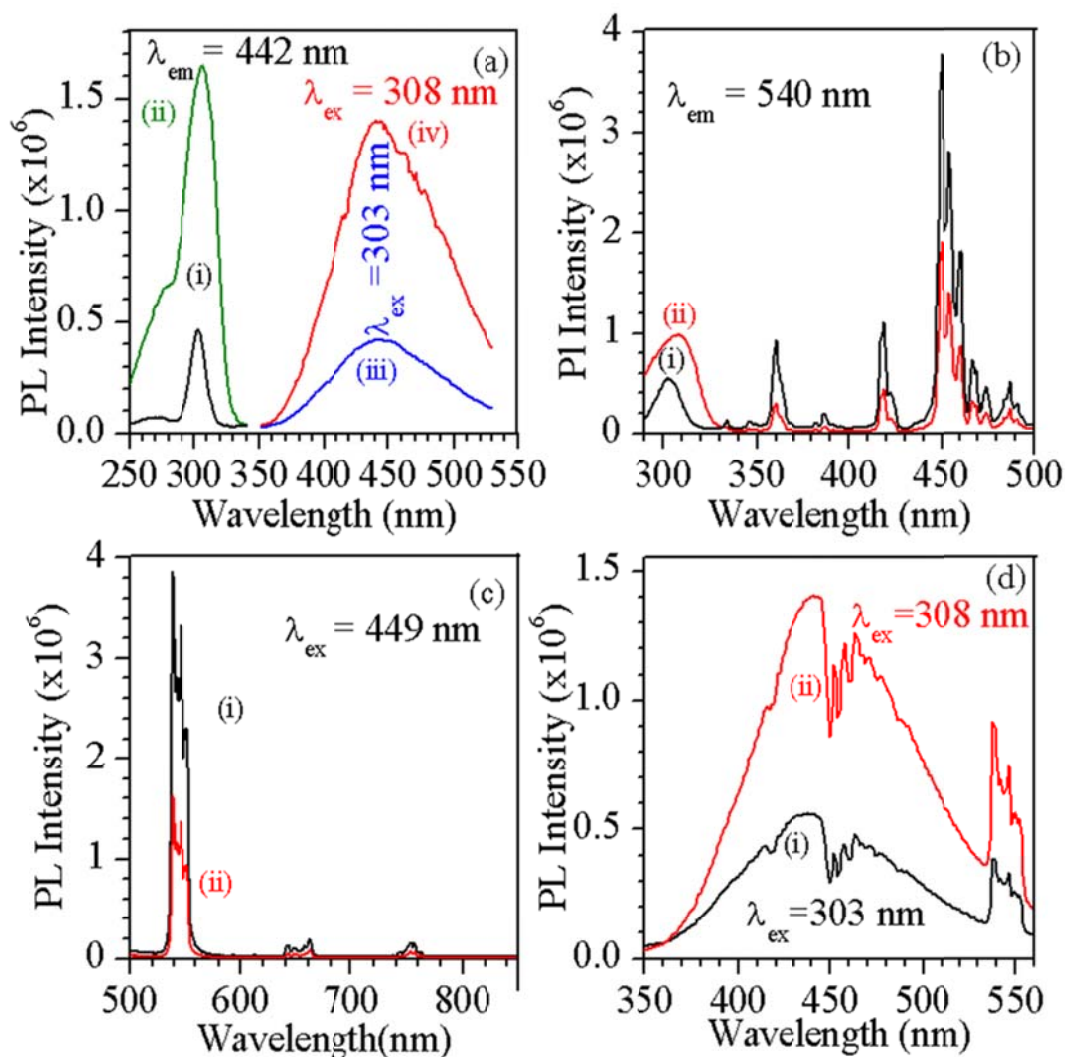


Figure 3: (a) PL excitation spectra of: (i) GdNbO_4 and (ii) $\text{Gd}_{0.99}\text{Bi}_{0.01}\text{NbO}_4$ monitored at $\lambda_{\text{em}} = 442$ nm, PL emission spectra of: (iii) GdNbO_4 and (iv) $\text{Gd}_{0.99}\text{Bi}_{0.01}\text{NbO}_4$ recorded at $\lambda_{\text{ex}} = 303$ and 308 nm, respectively. (b) PL excitation spectra of (i) $\text{Gd}_{0.93}\text{Ho}_{0.02}\text{Yb}_{0.05}\text{NbO}_4$ and (ii) $\text{Gd}_{0.92}\text{Bi}_{0.01}\text{Ho}_{0.02}\text{Yb}_{0.05}\text{NbO}_4$ recorded at $\lambda_{\text{em}} = 540$ nm. (c) PL emission spectra of (i) $\text{Gd}_{0.93}\text{Ho}_{0.02}\text{Yb}_{0.05}\text{NbO}_4$ and (ii) $\text{Gd}_{0.92}\text{Bi}_{0.01}\text{Ho}_{0.02}\text{Yb}_{0.05}\text{NbO}_4$ recorded at $\lambda_{\text{ex}} = 449$ nm. (d) PL emission spectra of (i) $\text{Gd}_{0.93}\text{Ho}_{0.02}\text{Yb}_{0.05}\text{NbO}_4$ and (ii) $\text{Gd}_{0.92}\text{Bi}_{0.01}\text{Ho}_{0.02}\text{Yb}_{0.05}\text{NbO}_4$ recorded at $\lambda_{\text{ex}} = 303$ (308) nm.

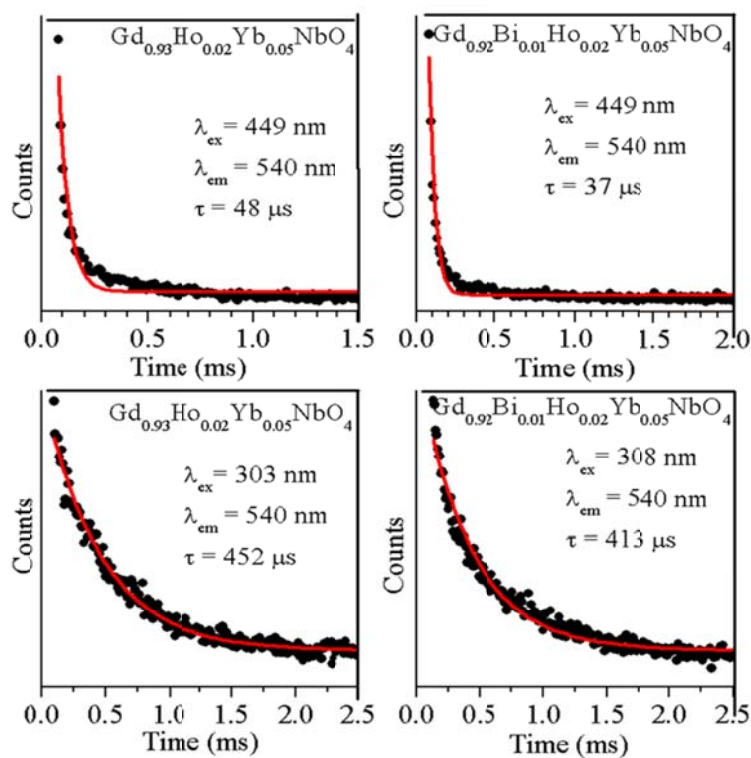


Figure 4: TRPL decay profile of $\text{Gd}_{0.93}\text{Ho}_{0.02}\text{Yb}_{0.05}\text{NbO}_4$ and $\text{Gd}_{0.92}\text{Bi}_{0.01}\text{Ho}_{0.02}\text{Yb}_{0.05}\text{NbO}_4$ recorded at $\lambda_{\text{ex}} = 449$ nm, 303 (308) nm and $\lambda_{\text{em}} = 540$ nm.

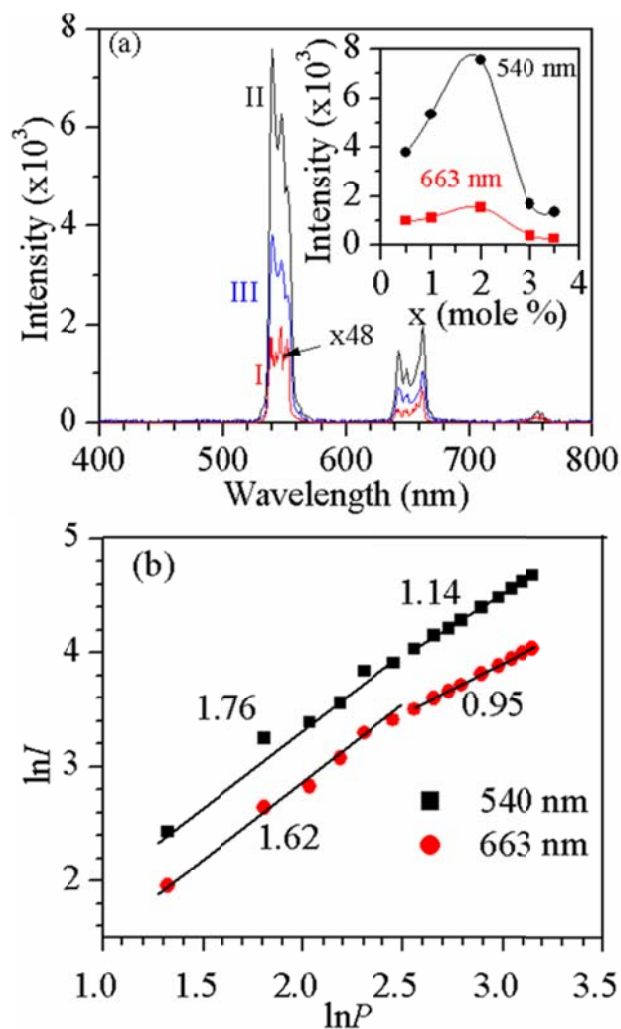


Figure 5: (a) UC emission spectrum of: (I) $\text{Gd}_{0.98}\text{Ho}_{0.02}\text{NbO}_4$, (II) $\text{Gd}_{0.93}\text{Ho}_{0.02}\text{Yb}_{0.05}\text{NbO}_4$ and (III) $\text{Gd}_{0.92}\text{Bi}_{0.01}\text{Ho}_{0.02}\text{Yb}_{0.05}\text{NbO}_4$ recorded at $\lambda_{\text{ex}} = 980$ nm. Inset to the Fig 5(a) shows UC emission intensities corresponding to 540 nm and 663 nm peaks in $\text{Gd}_{(0.95-x)}\text{Ho}_x\text{Yb}_{0.05}\text{NbO}_4$ as a function of Ho^{3+} ion concentration. (b) The $\ln I$ (intensity of UC emission) versus $\ln P$ (applied laser input power) plot. The slope of these curves (n) gives the number of photons involved in a particular UC process of different bands.

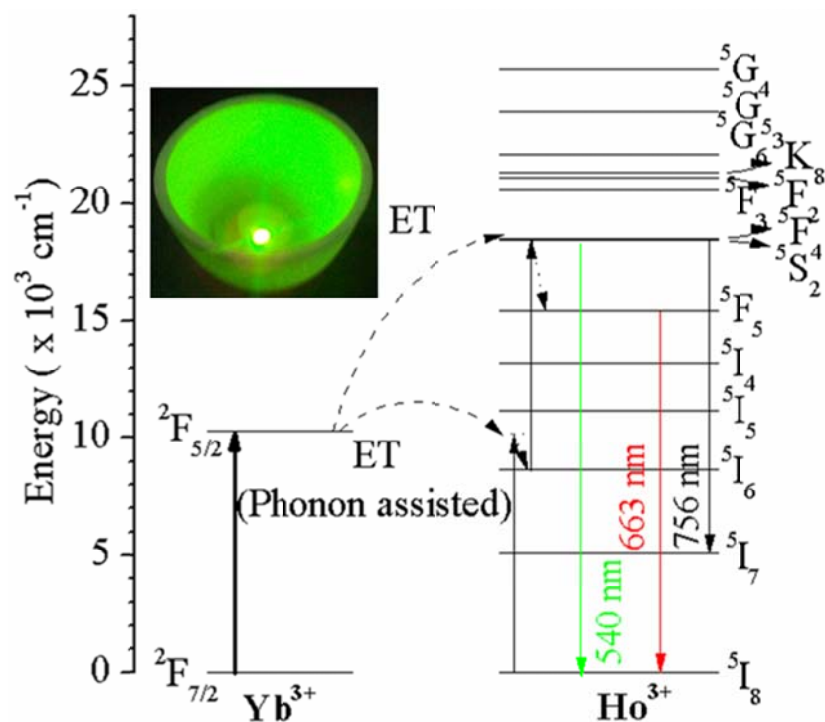


Figure 6: Schematic energy level diagram showing the mechanism involved in the UC emissions. Inset to the Fig. shows digital photograph of $\text{Gd}_{0.93}\text{Ho}_{0.02}\text{Yb}_{0.05}\text{NbO}_4$ phosphor under 980 nm laser excitation.

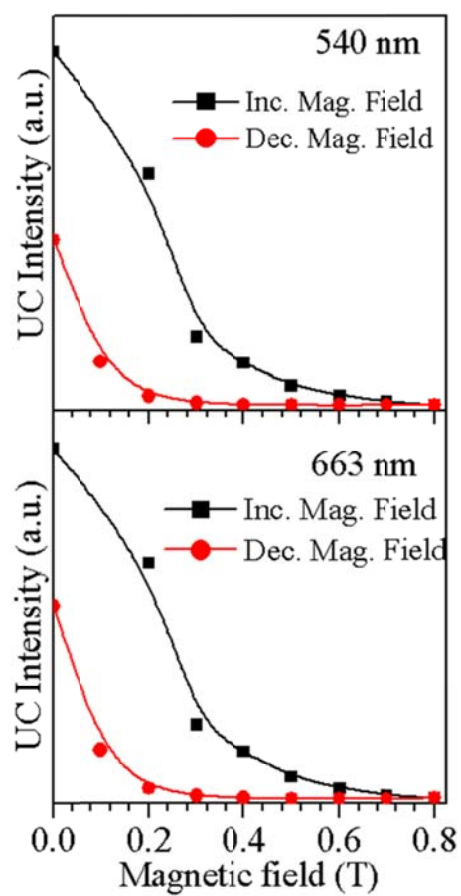


Figure 7: Effect of magnetic field on UC emission of $\text{Gd}_{0.93}\text{Ho}_{0.02}\text{Yb}_{0.05}\text{NbO}_4$ phosphor.